

Investigation of interstitial clustering in Al following electron irradiation at low temperature

J. B. Roberto,* B. Schoenfeld, and P. Ehrhart

Institut für Festkörperforschung der Kernforschungsanlage Jülich, D 5170 Jülich, Germany

(Received 28 December 1977)

The clustering of interstitials in Al has been investigated by x-ray diffuse scattering during an isochronal annealing program following electron irradiation at ~ 5 K. Measurements of the specific resistivity, volume relaxation, and lattice-parameter change before annealing are in satisfactory agreement with previous results for Frenkel defects in Al. The annealing data indicate that single interstitials migrate at the end of Stage I (~ 36 K) and a statistical distribution of di-, tri-, and tetra-interstitials is produced, which remains somewhat stable from 38 to 44 K. There is evidence that the di-interstitial migrates in Stage II₁ (~ 45 K) and a new cluster size distribution consisting mostly of 3–6 interstitials results. This distribution is stable from 50 to 55 K. Above 55 K, the clusters resume growth attaining a maximum size of 12–25 interstitials per cluster at 100–160 K. The observed cluster sizes following single and di-interstitial migration are consistent with the predictions of a simple kinetic model for diffusion annealing.

I. INTRODUCTION

The clustering of interstitials in irradiated metals is an important consideration in the overall description of radiation damage. For small defect clusters, the most direct information on the symmetry and size of the clusters is obtained from diffuse-scattering experiments.¹ Measurements close to the Bragg peak (Huang scattering) are sensitive to the cluster sizes and the symmetry of their long-range strain field, whereas measurements between the Bragg peaks² yield information on atomic displacements in the vicinity of the defects. The Huang scattering of x rays from interstitial clusters has been recently investigated in a variety of metals,¹ and the general evolution of clustering during annealing of electron-irradiated Al (Ref. 3) and Cu (Ref. 4) has been observed. In the present work, the results of a more detailed Huang-scattering study of interstitial clustering in Al are reported. This study was motivated primarily by the availability of improved theoretical descriptions⁵ of multiple interstitials in fcc metals as well as anelastic after-effect measurements⁶ for small clusters in Al, both of which provide additional data which can be correlated with the diffuse scattering.

In the experiment, an Al single crystal was irradiated at ~ 5 K with 3-MeV electrons to a defect concentration of $\sim 4 \times 10^{-4}$. Huang scattering intensities were measured following the irradiation at 5 K, and during an isochronal annealing program from 36 to 190 K. The 5-K data were combined with measurements of the lattice-parameter change and electrical resistivity on the same sample to yield values of the specific resistivity and volume relaxation for Frenkel defects in Al. In the annealing program, particular attention was given to the temperature region 36–55 K where

the initial stages of interstitial clustering are observed.³ From the annealing results, effective cluster sizes as a function of annealing temperature were determined and are compared with the predictions of a simple kinetic model for diffusion annealing.⁷

II. THEORY

The scattering results were interpreted using the well-established theory of the diffuse scattering from point defects and defect clusters in metals.^{8,9} For a statistical distribution of defects, the Huang scattering cross section is given by

$$S_H = c \left(\frac{h}{q} \right)^2 \left(\frac{fe^{-M}}{V_a} \right)^2 (\gamma^{(1)}\pi^{(1)} + \gamma^{(2)}\pi^{(2)} + \gamma^{(3)}\pi^{(3)}), \quad (1)$$

where c is the defect concentration, h is the nearest reciprocal-lattice vector, q is the distance from the corresponding reciprocal-lattice point, and fe^{-M} and V_a are the atomic-scattering factor and atomic volume, respectively. The γ 's are functions of the elastic constants and the directions of h and q , and the π 's are related to the dipole force tensor of the defects. Additional details are given elsewhere.^{3,8,9} The distinguishing feature of the Huang scattering is the proportionality to q^{-2} .

For point defects in Al, $\pi^{(2)}$ and $\pi^{(3)}$ (which are related to the deviation of the long-range strain field from cubic symmetry) are essentially zero. The quantity $\pi^{(1)}$ characterizes the strength of the defect, and is also related to the lattice-parameter change

$$\frac{\Delta a}{a} = \frac{1}{3} c \frac{\Delta V}{V_a} = c \frac{(\frac{1}{3}\pi^{(1)})^{1/2}}{V_a(C_{11} + C_{12})}, \quad (2)$$

where ΔV is the relaxation volume per defect and

C_{11} and C_{12} are elastic constants of the medium. A combination of measurements of S_H and $\Delta a/a$ therefore leads to a determination of the absolute concentration and volume relaxation of the defects. This simple result is somewhat complicated by the presence of both vacancies and interstitials in the sample. The lattice parameter change is proportional to the sum $\Delta V_i + \Delta V_v$, whereas S_H is proportional to the sum of the squares $\Delta V_i^2 + \Delta V_v^2$. In most cases, the vacancy contribution to the diffuse scattering can be neglected. However, even small values of ΔV_v can have a significant effect on the determination of $\pi^{(1)}$, c , and ΔV_i since ΔV_v enters the lattice-parameter change linearly.

Assuming that long-range strain fields for individual defects superpose linearly when the defects are in clusters, we can rewrite Eq. (1) for clusters as^{8,9}

$$S_H^{c1} = n S_H, \quad (3)$$

where the same concentration of point defects is now in clusters of number size n . The assumption of superposition is equivalent to assigning the same relaxation volume to point defects in clusters as for single defects. Recent model calculations⁵ for multiple interstitials in fcc metals estimate reductions in ΔV_i per interstitial varying from 5%–7% for the di-interstitial to 15%–20% for the tetra-interstitial. Equation (3) also assumes that the contribution of $\pi^{(2)}$ and $\pi^{(3)}$ to the S_H^{c1} can be neglected which is the case for scattering in the radial direction (q parallel to h) in Al.³

The proportionality of S_H^{c1} to n provides a simple means to determine the cluster size if ΔV_i^{c1} and the concentration are known. The electrical resistivity is a convenient measure of relative defect concentration, but additional uncertainties due to possible changes of point defect resistivities when the defects are in clusters must be considered. For Al, the resistivity change $\Delta\rho$ is proportional to $\Delta a/a$ to within a few percent over the temperature range of our measurements,¹⁰ and therefore only the relative change in ΔV_i upon clustering enters into the size determination. Neglecting second order terms in ΔV_v , the cluster size as a function of annealing temperature becomes

$$n(T) = S_H^T \Delta\rho \Delta V_i / S_H \Delta\rho_T \Delta V_i^T, \quad (4)$$

where S_H , $\Delta\rho$, and ΔV_i are values prior to clustering and ΔV_i^T is the relaxation volume per interstitial in clusters of size n . For a distribution of cluster sizes, n is an effective number of interstitials per cluster, where the various cluster sizes have been weighted according to the relative

concentration of single interstitials in clusters of that size [see Eq. (3)].

III. EXPERIMENT

The experimental procedure was similar to that of the previous Al study³ and will be only briefly described here. A rectangular platelet (0.8×2 cm) was spark cut from a high-purity Al single crystal and electrolytically thinned to ~ 100 μm . The sample had a (111) surface and was mounted so that the (220) reflection could also be measured in symmetrical transmission. Wire resistivity leads were soft soldered directly to the sample edges. The mounted sample had a mosaic spread of $\sim 0.2^\circ$ and a residual resistivity ratio of ≥ 4000 .

The irradiation was carried out at the Jülich low-temperature irradiation facility¹¹ using 3-MeV electrons at a current density of ~ 20 $\mu\text{A}/\text{cm}^2$. The total induced-resistivity change was 128 n Ω cm. The irradiation was uniform over the sample dimensions to better than $\pm 5\%$ as estimated from the measured beam profiles. During irradiation, the sample was cooled in a continuous stream of liquid He. The transfer to the x-ray cryostat was also accomplished with the sample immersed in liquid He.

The x-ray measurements were performed using an apparatus which has been previously described³ and consists of a 6-kW rotating-anode x-ray tube, a focusing monochromator, and an x-ray cryostat where the sample temperature could be varied from 4 to 300 K. The sample was positioned at the focus of the monochromator, and an overall resolution of approximately 0.1° in the diffraction plane and 1.4° vertically was used for most of the measurements. Huang scattering intensities were determined relative to a monitor counter on the primary beam, and absolute intensities were measured using a polystyrene standard.¹² All x-ray measurements were performed at 5 K using Cu $K\alpha_1$ radiation.

Huang diffuse scattering intensities were measured near the (222) reflection in the [111] and $[1\bar{1}0]$ directions, near the (220) in the [110] and $[1\bar{1}1]$ directions, and near the (111) in the $[1\bar{1}0]$ direction. The Huang intensities were determined by subtracting the background scattering following complete annealing of the defects. These background measurements agreed well with corresponding measurements prior to the irradiation. For the (220) transmission measurements, Huang intensities from two different positions on the sample agreed to better than 10% after appropriate thickness corrections. The scattering data were corrected for the finite resolution of the diffractometer by assuming a distribution of intensity on

Huang spheres for single interstitials and spherically symmetric for clusters. These corrections were as large as a factor of ~ 2 at the smallest q values but became negligible for $q/h \geq 0.03$.

Lattice-parameter measurements were made on the sample before and after irradiation and after complete annealing using the Bond¹³ technique at the (333) reflection. Measurements at eight different positions on both sides of the crystal agreed to $\sim 10\%$ in $\Delta a/a$, which is close to the instrumental error and confirms the uniformity of the irradiation.

The annealing program consisted of 15-min annealing pulses at successively higher temperatures followed by measurements of the diffuse scattering at 5 K. The corresponding resistivity change was measured at 4.2 K with the sample in liquid He. Temperatures were determined using a carbon resistor up to 75 K and a thermistor above. Absolute temperatures are probably accurate to 2 K in the temperature range 36–55 K and to 5 K above. Relative temperatures are more accurately known (~ 0.5 K at 55 K). The temperature scales for the diffuse scattering and resistivity annealing are obviously identical since these measurements were performed on the same sample.

During the data analysis, a discrepancy of $\sim 25\%$ was noticed between the absolute intensity data for the (220) and (222) reflections. This discrepancy was traced to a slight bending of the sample which probably occurred during mounting. The bending resulted in a reduced intensity at the (222), a corresponding effect at the (220) is unlikely since this would require a bending of the sample about its (111) surface normal. Relative intensities for the (220) and (222) were in excellent agreement over the range of the annealing and were obviously not affected. The absolute intensity at the (222) could be adjusted in comparison with fine-resolution measurements made at several points in the annealing program. These measurements were made with a restricted beam height so that the bending could be neglected. A correction factor of ~ 1.2 derived from these measurements correlated well with the absolute intensity discrepancy and has been applied to the (222) data. It should be emphasized that these considerations do not affect the clustering results where only relative intensities are needed.

IV. RESULTS

The general features of the diffuse scattering observed in the present experiment are consistent with previous results for Al which have been described in detail elsewhere.³ In Fig. 1, some ty-

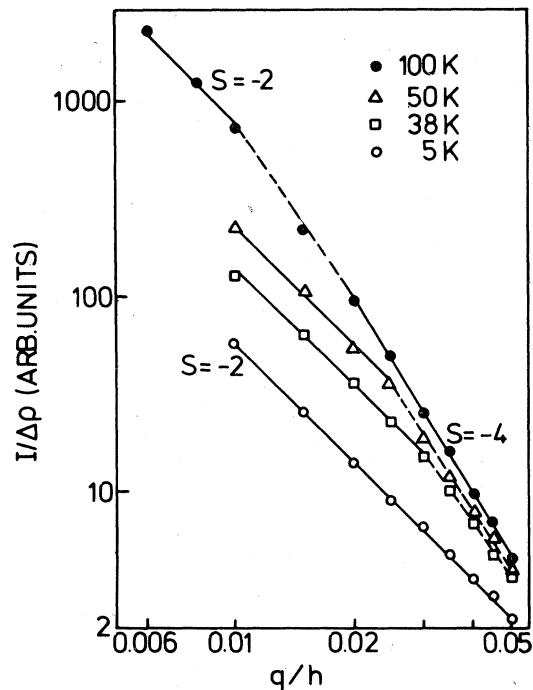


FIG. 1. Symmetric diffuse scattering curves for the radial direction in the vicinity of the (222) reflection at 5 K and after several points in the annealing program. The intensities are normalized to the same Frenkel defect concentration using the electrical resistivity.

pical diffuse-scattering curves for measurements in the radial (q parallel to h) direction in the vicinity of the (222) reflection are shown. These curves have been normalized to the same point defect concentration using the electrical resistivity. Following the irradiation, the Huang scattering (q^{-2}) region extends to quite large values of q as expected for single defects. Upon annealing, the normalized scattering cross section increases, and the Huang region collapses toward the Bragg peak and is replaced at large q by an asymptotic scattering⁹ where the cross section varies as q^{-4} . These observations are consistent with the formation of defect clusters in the sample.

The overall results are summarized in Fig. 2, where Huang intensities for the (111), (220), and (222) reflections can be compared with the recovery of the electrical resistivity. The Huang intensities for both the radial and perpendicular directions have been normalized to the 5-K radial value for each reflection. For the radial direction, the normalized intensities first decrease with the electrical resistivity, indicating a reduction in defect concentration by recombination reactions. At 38 K, clustering occurs abruptly as indicated by the sharp increase in the Huang in-

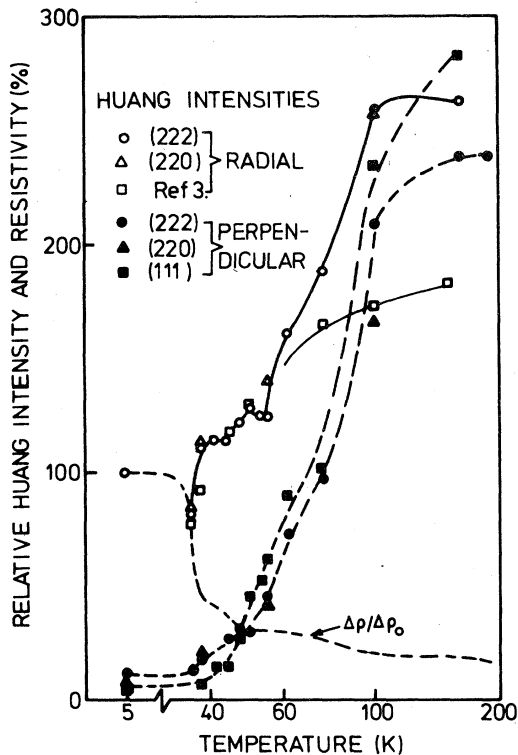


FIG. 2. Relative Huang scattering intensity and resistivity change as a function of annealing temperature. For a given reflection, the Huang scattering data are normalized to the corresponding 5 K value for the radial direction.

tensity as compared to the resistivity. This is followed by regions of slower intensity growth (38–55 K) and rapid growth (62–100 K) until the maximum intensity is reached at 100–160 K. The radial scattering data for the (222) and (220) reflections are in good agreement over the range of the annealing. Relative intensities are accurate to about 5% up to 55 K, but are subject to increasing errors due to a restricted Huang region

above 62 K.

For the perpendicular direction, the Huang intensity is close to zero before the onset of clustering, and then increases somewhat smoothly to become comparable to the radial scattering at ~100 K. The perpendicular results are subject to somewhat larger errors due to the low scattering intensity at the beginning of the annealing program and a Huang region which is further restricted by interference from the Bragg peak at the (220) and (222). The observation of near-zero intensity in the perpendicular direction before annealing is consistent with the presence of a defect with cubic or tetragonal symmetry as has been reported earlier for the single interstitial in Al.³ The large values of the perpendicular scattering at higher annealing temperatures (~100 K) indicates that the larger interstitial clusters are probably dislocation loops.

The Huang intensities observed in the present experiment are in satisfactory agreement with previously published³ results for Al. For comparison, radial intensities from the earlier experiment have also been included in Fig. 2. The agreement between the two experiments is quite good below 75 K. For higher annealing temperatures, the low intensities from the earlier work may be explained by the somewhat lower resolution and broader crystal mosaic spread in that experiment which did not allow the reliable evaluation of the data close to the Bragg peak. The recovery of the electrical resistivity in the present experiment is also in good agreement with previously reported results^{3,6} for similar irradiations of Al.

For single interstitials at 5 K, the Huang scattering and resistivity data were combined with measurements of the lattice-parameter change on the sample to obtain absolute values for the interstitial relaxation volume ΔV_i , the resistivity change ρ_F per Frenkel defect, and the strength of the defects as measured by the trace of the dipole

TABLE I. Absolute quantities for Frenkel defects in Al.

Measurement		$\frac{\Delta a/a}{\Delta \rho}$ ($10^3/\Omega$ - cm)	ρ_F ($\mu\Omega$ - cm/at.%)	TrP (eV)	$\frac{\Delta V_i}{V_a}$
Huang scattering ^a plus $\Delta a/a$	Present work	1.77 ± 0.17	3.2 ± 0.6	42 ± 4	1.7 ± 0.3
	Ref. 3	1.61 ± 0.10^b	3.9 ± 0.6	47 ± 4	1.9 ± 0.2
Scattering between the Bragg peaks	Ref. 2		4.2 ± 0.8		1.9 ± 0.2

^aHuang scattering results for ρ_F , TrP, and $\Delta V_i/V_a$ assume $\Delta V_v=0$.

^bTaken from Ref. 10.

tensor [$\text{Tr}P = (3\pi^{(1)})^{1/2}$]. The present results are compared with previously published data for Al in Table I. For the present and previous³ Huang scattering studies, the differences in ρ_F , $\text{Tr}P$, and $\Delta V_i/V_a$ result primarily from the different values of $\Delta a/a$ used in the two experiments. The uncertainty in $\Delta a/a$ enters the determination of the absolute concentration quadratically and accounts for most of the estimated error in the Huang scattering results in Table I. Values for ρ_F and $\Delta V_i/V_a$ derived from diffuse-scattering measurements² between the Bragg peaks are also shown in Table I and are consistent with the Huang scattering results.

The combined Huang scattering and lattice-parameter results in Table I assume that the vacancy contribution to these data can be neglected. This is not unreasonable if $\Delta V_v \approx -0.05V_a$ as indicated recently² in Al by small-angle x-ray scattering. If, on the other hand, $\Delta V_v \approx -0.38V_a$ as determined from quenching studies¹⁴ is assumed, the present Huang scattering results for ρ_F , $\text{Tr}P$, and $\Delta V_i/V_a$ change significantly to $\sim 1.0 \mu\Omega \text{ cm/at.}\%$, 25 eV, and 0.9, respectively. While these values are inconsistent with the results of the diffuse-scattering measurements between the Bragg peaks, it is clear that a major uncertainty in the determination of these absolute quantities from combined Huang-scattering and lattice-parameter measurements is due to ΔV_v . Accordingly, the present results cannot improve the overall accuracy of ρ_F , $\text{Tr}P$, and ΔV_i . The relative agreement between the present and earlier Huang-scattering results is a good indication that relative errors in the combination of diffuse-scattering, lattice-parameter, and resistivity measurements are not significant in these data. The over-

all 5-K results also establish the presence of a statistical distribution of single interstitials in our sample before annealing.³

For the clustering results, the radial Huang intensities were divided by the corresponding resistivity change to determine the effective number of interstitials per cluster as a function of annealing temperature. These results are shown in Fig. 3 along with the resistivity recovery and will be discussed in detail in Sec. V. The appropriate stage-boundary temperatures for the recovery of electron-irradiated Al are also indicated in Fig. 3. The relative accuracy of the effective sizes (neglecting possible changes in ΔV_i upon clustering) is better than 10% up to 55 K and increases to $\sim 20\%$ at 100 K. The present data below 75 K are in good agreement with earlier results³ for Al where a less complete annealing program was reported.

V. DISCUSSION

In this section, the general features of the clustering of interstitials in Al will be discussed in terms of the annealing results (Fig. 3). Single interstitials survive to ~ 36 K where long-range migration occurs and a distribution of multiple interstitials of effective size ~ 2.5 quickly develops near the end of stage I (~ 38 K). Including estimates for the change in the interstitial relaxation volume upon clustering,⁵ the effective size at 38 K becomes ~ 2.8 . This is consistent with the presence of $\sim 30\%$ tri-interstitials in the sample.

From 38 to 44 K, a somewhat stable region of slow cluster growth is observed. The di-interstitial does not migrate freely in this region, otherwise cluster sizes much greater than 3 would be expected. On the other hand, some agglomeration of defects does occur, perhaps by stress-induced reactions. These effects would not be unexpected at cluster concentrations of $\sim 10^{-4}$ as present in the sample at 38 K. An alternative explanation would be to associate some of this growth with the completion of single interstitial annealing (if it is not complete at 38 K).

The increase in cluster growth rate in the temperature range 44–50 K suggests that the di-interstitial migrates in this region. This is consistent with the observed effective cluster size at 50 K of ~ 4 (~ 5 including the estimated relaxation change). This is just the temperature region of stage II_1 in the resistivity which has been previously attributed to di-interstitial migration.^{3,6}

The effective cluster sizes following single and di-interstitial migration can be correlated with the predictions of a simple kinetic model for diffusion annealing.⁷ In this model, the size distri-

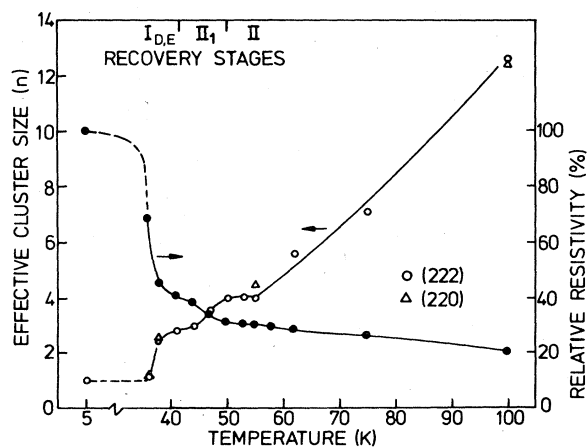


FIG. 3. Effective number of interstitials per cluster as a function of annealing temperature. The resistivity recovery with its principal stages is also shown.

TABLE II. Estimated sizes for interstitial clusters after diffusion annealing of single and di-interstitials in Al.

Cluster size (n)	2	3	4	5	6-8	Effective size ^a	
						Theory	Experiment ^b
Single-interstitial annealing							
Cluster fraction	0.67	0.26	0.07		
Interstitial fraction	0.55	0.33	0.12	2.6	~3 (40 K)
Di-interstitial annealing							
Cluster fraction	...	0.31	0.35	0.22	0.11		
Interstitial fraction	...	0.23	0.34	0.27	0.16	4.4	~5 (50 K)

^a Average cluster size per unit concentration interstitials [(see Eq. (3))].

^b Includes estimated changes in ΔV_i upon clustering (see text and Ref. 5).

bution of interstitial clusters upon completion of diffusion annealing is obtained from generalized Waite equations.¹⁵ Predicted distributions and effective sizes following single and di-interstitial migration are given in Table II. These results are based on the assumption that the interstitial reaction radii r_i are independent of cluster size; the effective sizes increase up to 20% if $r_i \sim n$ is assumed. The results for di-interstitials are estimated assuming that reactions at vacancies and subsequent clustering reactions involving single and di-interstitials proceed sequentially. The estimated effective size increases to 5.6 if tri-interstitials are also allowed to migrate. The predicted effective sizes are consistent with the observed sizes following stages $I_{D,E}$ and II_1 and therefore support the assignment of these stages to single and di-interstitial migration, respectively. The simultaneous migration of tri-interstitials in stage II_1 cannot be ruled out. These results must be viewed qualitatively in the light of the above approximations and since the model calculations are strictly valid only for low-defect concentrations. Nevertheless, it is not expected that the branching ratios between various clustering reactions would be significantly changed at higher concentrations.

The estimated size distributions in Table II can also be correlated with the results of a recent study⁶ of anelastic relaxation processes due to small interstitial clusters in Al. In this work, the authors attribute their process *A* which anneals at 38 K and process *B* which anneals at 47 K to the simultaneous reorientation and migration of single and di-interstitials, respectively. This is consistent with the disappearance of single and di-interstitials in stages $I_{D,E}$ and II_1 , respectively as inferred from the present experiment. Another process (process 2) which also anneals at 47 K is assigned to the reorientation without

migration of the tri-interstitial. This would suggest that di- and tri-interstitial migration occur simultaneously. On the other hand, the present experimental results can also be adequately explained by invoking only di-interstitial migration in stage II_1 . In this case, additional relaxation peaks⁶ (processes 0 and 4) which are activated from 38-60 K might be associated with tri- (and tetra-) interstitials.

Following di-interstitial migration in stage II_1 , the effective cluster size is stable from 50 to 55 K. This is not surprising if there are no freely migrating defects in this temperature range. The cluster density in the sample is reduced to $\sim 2 \times 10^{-5}$ by 50 K, which is probably low enough to suppress the stress-induced interactions which may be responsible for the slow growth after single interstitial migration. The stable cluster size from 50 to 55 K is consistent with the small decrease in the resistivity and the observed stability of the anelastic processes 0 and 4 in this range.⁶ On the other hand, the perpendicular scattering does change in this region, increasing from 0.3 of the radial scattering at 50 K to 0.4 at 55 K (Fig. 2). This suggests a configurational change for some of the clusters, perhaps into a form which can subsequently grow as dislocation loops.

Above 55 K, cluster growth resumes and a maximum effective size of $\sim 12-25$ interstitials per cluster is attained at 100-160 K. The smaller number results from assuming that the relaxation volume for interstitials in clusters is the same as for single interstitials, and larger number assumes an interstitial relaxation volume of 1 at. volume as expected for large dislocation loops. The actual effective size lies between these values, perhaps near 20. The nature of the clusters can be inferred from the ratios $\pi^{(2)}/\pi^{(1)}$ and $\pi^{(3)}/\pi^{(1)}$ which reflect the deviation of the long-range

strain field from cubic symmetry. A unique determination of $\pi^{(2)}$ and $\pi^{(3)}$ was not possible in this experiment since these quantities do not appear independently in the scattering equations for the reflections measured. Nevertheless, the comparable value of the perpendicular and radial scattering at 100–160 K is consistent with the presence of dislocation loops.³

Although the coarseness of the annealing program above 55 K does not allow a detailed interpretation of the cluster growth in this region, it is interesting to speculate on the possibility of additional structure in the growth curve which could be associated with the clustering process or the migration of higher multiple interstitials. The annealing of two anelastic processes⁶ for multiple

interstitials in Al near 60 K as well as the existence¹⁶ of two additional intrinsic substages (at 74 and 82 K) in the stage II recovery of electron-irradiated Al are suggestive of the possibility of such effects.

ACKNOWLEDGMENTS

The authors gratefully acknowledge helpful discussions with W. Schilling, K. Sonnenberg, K.-H. Robrock, K. Schroeder, H. R. Schober, and H. Trinkaus as well as the experimental assistance of J. Kozłowski. One of us (J.B.R.) wishes to thank Professor Schilling and the members of the Institut für Festkörperforschung for their hospitality during his stay in Jülich.

*Permanent address: Solid State Division, Oak Ridge National Laboratory, Oak Ridge, Tenn. 37830.

¹See, P. Ehrhart, *J. Nucl. Mater.* **69/70**, 200 (1978) and B. C. Larson, in *Fundamental Aspects of Radiation Damage in Metals*, edited by M. T. Robinson and F. W. Young, Jr. USERDA Rep. CONF-751006, (unpublished), p. 820, for recent reviews.

²H.-G. Haubold, in *Fundamental Aspects of Radiation Damage in Metals*, edited by M. T. Robinson and F. W. Young, Jr. USERDA Rep. CONF-751006, (unpublished), p. 268.

³P. Ehrhart and W. Schilling, *Phys. Rev. B* **8**, 2604 (1973).

⁴P. Ehrhart and U. Schlagheck, *J. Phys. F* **4**, 1589 (1974).

⁵H. R. Schober, *J. Phys. F* **7**, 1127 (1977).

⁶K.-H. Robrock, L. E. Rehn, V. Spirić, and W. Schilling, *Phys. Rev. B* **15**, 680 (1977); V. Spirić, L. E. Rehn, K.-H. Robrock, and W. Schilling, *ibid.* **15**, 672 (1977).

⁷K. Schroeder, *Radiat. Eff.* **17**, 103 (1973).

⁸P. H. Dederichs, *J. Phys. F* **3**, 471 (1973).

⁹H. Trinkaus, *Phys. Status Solidi B* **54**, 209 (1972).

¹⁰H. Wagner, F. Dworschak, and W. Schilling, *Phys. Rev. B* **2**, 3856 (1970).

¹¹J. Hemmerich, W. Sassin, and W. Schilling, *Z. Angew. Phys.* **29**, 1 (1970).

¹²C. J. Sparks and B. Borie, in *Local Atomic Arrangements Studied by X-ray Diffraction*, Metallurgy Society Conf. No. 36 (Gordon and Breach, New York, 1966).

¹³W. L. Bond, *Acta Crystallogr.* **13**, 814 (1960).

¹⁴R. M. Emrick and P. B. McArdle, *Phys. Rev. B* **3**, 188 (1969).

¹⁵T. R. Waite, *Phys. Rev.* **107**, 463 (1957).

¹⁶W. Schilling, G. Burger, K. Isebeck, and H. Wenzl, in *Vacancies and Interstitials in Metals*, edited by A. Seeger, D. Schumacher, W. Schilling, and J. Diehl (North-Holland, Amsterdam, 1970), p. 255.